Performance Improvement of UV Photodetectors using Cd-doped ZnO Nanostructures

Fatemeh Abbasi
Malek-Ashtar University of Technology
Fahimeh Zahedi (zahedy2001@gmail.com)
Malek-Ashtar University of Technology https://orcid.org/0000-0002-2152-5610
Mohammad hasan Yousefi
Malek-Ashtar University of Technology

Research Article

Keywords: ZnO, ZnO:Cd, UV photodetector, thermal decomposition, photoresponse

Posted Date: March 31st, 2021

DOI: https://doi.org/10.21203/rs.3.rs-328527/v1

Performance improvement of UV photodetectors using Cd-doped ZnO nanostructures

Fatemeh Abbasi [a], Fahimeh Zahedi [a,*], Mohammad hasan Yousefi [a]
[a] *Nano Physics Center, Department of Physics, Malek-Ashtar University of Technology, Shahin Shahr Esfahan 83145/115, Iran*

Abstract
The present research performed thermal decomposition to synthesize pure zinc oxide (ZnO) and cadmium-doped ZnO (ZnO:Cd) nanorods with ZnO to Cd weight ratios of 93:7, 95:5 and 97:3. Field emission scanning electron microscopy (FESEM), X-ray diffraction (XRD) and photoluminescence (PL) spectroscopy were performed and current/voltage and current/time measured to determine the optical, structural and morphological characteristics of ZnO and ZnO:Cd. The XRD results suggested the hexagonal wurtzite structure of all the samples and the successful incorporation of Cd into the ZnO structures. This incorporation caused a spherical to rod-like change in the shape of the nanostructures. An intense and sharp peak was observed at 380 nm (3.26 eV) in the UV region of the PL spectra of all the samples. A UV photodetector fabricated on the basis of ZnO and ZnO:Cd nanorods with a metal-semiconductor-metal configuration showed the significant photocurrent and photosensitivity of the ZnO:Cd samples in the UV photodetection application. The sensitivity of the fabricated ZnO photodetectors with Cd percentages of 0, 3, 5 and 7% was respectively obtained as 110.62, 463.28, 762.40 and 920.30. The fastest photoresponse, with a rise and decay time of 2.5 and 4 s, respectively, was associated with the sample doped with 5% Cd.
Keywords: ZnO, ZnO:Cd, UV photodetector, thermal decomposition, photoresponse

1.Introduction

The military and civil applications of the ultraviolet (UV) technology include chemical and biological research, optical communication and measuring UV radiation and radiation from artificial sources [1]. In addition to the early detection of missiles, UV applications are growing in astronomy and distinguishing true from false targets. The bandgap of the materials used in these UV detectors should be broad and their UV penetration depth and resistance to UV radiation adequate. Specific precursors should be produced to construct this type of photodetector [1-4].

Given the large bandgap of ZnO at ambient temperature and its biocompatibility, mechanical and chemical stability and excition binding energy of as high as 60 meV, it can be used as an appropriate n-type semiconductor to produce UV photodetectors, whose first generation included thin ZnO layers and bulk materials [5]. The large surface-to-volume and aspect ratios of one-dimensional ZnO nanostructures make them appropriate for improving the performance of these detectors. The present findings suggested the high sensitivity of one-dimensional ZnO nanostructures to UV radiation and therefore changes in their conductivity. In addition to UV photodetection, ZnO can be applied to transparent electrodes, solar cells, laser, anti-reflection layers and light emitting diodes [5-8].

Various techniques utilized so far to improve the features of ZnO UV photodetectors include using composite materials, changing the morphology, resizing and doping, which is a commonly-used and efficient method in this regard [9- 11]. Research suggests doping

transition metals, including cadmium, nickel, cobalt, manganese and iron, into the ZnO lattic can enhance the electrical, magnetic and optical features of UV photodetectors based on ZnO nanostructures [12, 13]. Impacts of employing chromium-doped ZnO nanorods on UV photodetection were investigated by Safa et al [14]. Green/blue emissions and effects of copper doping on UV photosensitivity based on thin ZnO films were also investigated by Li et al [15]. Shabannia employed cobalt-doped ZnO nanorods to fabricate highly-sensitive UV photodetectors [11]. Moreover, Rajalakshmi et al. scrutinized the response of UV photodetectors based on ZnO nanostructures dope with transition metals such as manganese, nickel and cobalt [16]. In addition, the impact of iron, nickel and copper on UV photodetectors was investigated at various concentrations by Chu et al [17-19].

These reports suggest the challenges facing the development of ZnO UV photodetectors include fast relaxation and photocurrent saturation. The absorption and desorption of oxygen on the surface of ZnO nanostructures can decrease dark current and raise the sensitivity of ZnO photodetectors. This process, however, prolongs the rise and decay times of UV photodetectors and restricts the practical usafe of ZnO nanostructures [20-22]. Cd was proposed as a dopant to solve the problem cited and raise the photoresponse of UV detectors.

With promising optoelectronic properties, Cd can be utilized to fabricate devices based on ZnO given the increased absorption of oxygen molecules on the nanostructures surface in the dark as a result of increased defects in the donor caused by replacing Zn^{2+} with Cd^{2+} [23, 24]. Increases in the number of holes trapped by oxygen ions under UV radiation also increase the number of free electrons that contribute to producing the photocurrent [22]. Given that incorporating Cd into pure ZnO improves its conductivity and carrier concentration, ZnO:Cd can be used in photovoltaic applications such as protective layers, sensors and light emitting diodes of a UV type. The photovoltaic benefits of ZnO:Cd for optoelectronic devices have been reported in literature [25, 26]. In 2009, Purusothaman et al. explored the impact of Cd doping on the characteristics of ZnO nanostructures and reported a higher donor content such as oxygen vacancy in Cd doped ZnO nanorods than in pure ZnO. Replacing Zn^{2+} with Cd^{2+} raised defects in the donor, which increased the n-type carrier concentration of ZnO, Zn interstitial and oxygen vacancy sites [24]. ZnO nanostructures may therefore enhance the features of the material and parameters of photodetectors using Cd dopants.

The approaches utilized to synthesize pure and doped ZnO nanostructures include sputtering, spray pyrolysis, sol-gel, pulse laser deposition and hydrothermal and thermal decomposition [17, 24]. The simplicity of thermal decomposition and its high speed of producing pure cost-effective crystalline ZnO nanostructures using a single chemical agent and without employing a catalyst have turned this method into the most popular technique for producing ZnO [27]. Given these excellent properties, the present experiments were conducted to synthesize ZnO nanostructures using thermal decomposition.

The present research improved the performance of photodetectors by performing thermal decomposition based on Cd doping and synthesizing ZnO nanostructures with ZnO to Cd weight ratios of 93:7, 95:5 and 97:3. The results of investigating the optical, structural, electrical and morphological features of the samples were also presented.

2.Experimental

2.1 Powder products

Researchers seek to propose simple methods of developing one-dimensional zinc oxide nanostructures given that these tecqhniques fundamentally require an accurately-controlled synthesis environment, expensive equipment and time-consuming methods. In 2009, Lane et al. developed highly-pure ZnO nanowires through simple thermal decomposition of zinc acetate at 300 ˚C [28].

This study performed thermal decomposition to develop Cd-doped ZnO nanostructures through decomposition, deposition and evaporation. Not using catalysists differentiate thermal decomposition from the common vapor/liquid/solid mechanism. The ZnO:Cd nanostructures were synthesized using zinc acetate dehydrate ($Zn(CH_3COO)_2.2(H_2O)$, Merck) and cadmium acetate dehydrate ($Cd(CH_3COO)_2.2(H_2O)$, Merck) [22, 26]. cadmium and zinc concentrations were the only growth factors that were not kept the same for all the samples. These nanostructures were synthesized by pouring 3 g of zinc acetate dehydrate with cadmium acetate dehydrate weight ratios of 93:7, 95:5, 97:3 into alumina crucibles and mixing for one hour. The crucibles were then kept in an electric furnace for twelve hours. The temperature of the furnace increased to 300 ºC with a rate of 2.5 ºC/min and were then cooled down with a rate of 5 ºC/min. The empirical processes were repeated eight times to confirm the findings.

2.2 Device fabrication

Thin films of ZnO:Cd were synthesized at diverse ZnO-to-Cd ratios to explore the application of ZnO:Cd nanostructures to UV photodetectors. Forty ml of deionized water was then added to separate containers into which the powder produced by each crucible was poured in a way that different solutions with the same concentration was obtained. To ensure the homogeneity of the solutions in the containers, they were kept in an ultrasonic tank for twenty minutes. The potential of the powder as a UV photodetector was appraised by placing 3 drops of every solution on 1×15×15 mm^3 glass substrates, which were deposited with an aluminum layer as an electrode. Physical vapor deposition method was also performed to deposit this layer. The conductivity between the two sides was cut off by creasing a gap on the electrode by employing sharp blades. The samples were dried by being kept in a 100 ˚C oven for fifteen minutes after measuring the short conductivity using the high resistance between the two sides of the gap. The experiment and fabrication conditions of the layers and fabrication conditions of the electrical connection were the same for all the samples.

According to figure 1, a UV photodetector was fabricated through thermal decomposition and incorporation of the synthesized nanostructures between the two conductive areas, i.e. aluminum and the glass substrate as the insulation zone.

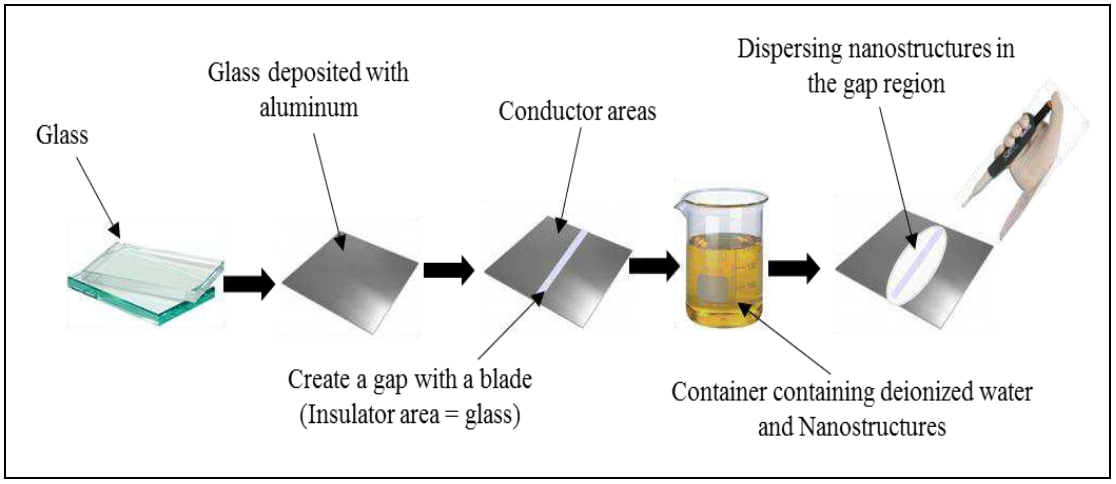

Fig. 1. Schematic structure of the UV photodetector [29].

Characterization of powder and device

An X-ray diffractometer (Stoe, Germany) with a copper anticathode was employed to investigate the crystal structure using a Cu kα wavelength of 1.54 Å at 20-90 degrees. FESEM (Hitachi S-4160) was performed to examine the powder morphology. A helium cadmium laser as an illumination source emitting at 325 nm was utilized to measure the photoluminescent (PL) properties of the nanostructures. Furthermore, a Keithley 2400 source meter was used to measure current-time (I-t) and current-voltage (I-V) specifications under dark and ambient illumination (UV light at 350 nm) conditions at ambient temperature and determine the impact of Cd doping on the performance of the UV photodetectors.

3. Results and Discussions

3.1 Structural properties

The XRD spectra obtained at various Cd concentrations in figure 2 to explore the structural characteristics of the ZnO and ZnO:Cd powder showed the peaks at (100), (002), (101), (102), (110), (103), (200), (112) and (201) for all the samples to correspond to that of the ZnO reference card (0704-076-01). The XRD results showed the hexagonal wurtzite structure of all the samples with an orientation of 002. No impurity and secondary phases associated with Cd, Cd oxide and other compounds were observed in the samples less than 5% Cd, which suggested that Cd^{2+} ions were completely dissolved in the ZnO lattice. The larger radius of Cd^{2+} ions (0.97 Å), which was replaced with the ionic places of Zn^{2+} ions with a radius of 0.74 A˚ resulted in a low displacement in the place of the sample peaks compared to the reference card [24]. The samples doped with over 5% weight of Cd^{2+} created a secondary or impure phase of $CdCO_3$ in the ZnO nanostructures. The highest (002) diffraction plane intensity was observed in the 5% Cd sample. Reductions in the (002) plane intensity, formation of a non-crystalline $CdCO_3$ phase and differences in the ionic radius between Cd^{2+} (0.97 Å) and Zn^{2+} (0.74 Å) deteriorated the crystalline quality of the nanostructures in the samples doped with over 5% weight of Cd^{2+}. Stress was therefore developed in the lattice and crystallinity of the nanostructures reduced [23, 24].

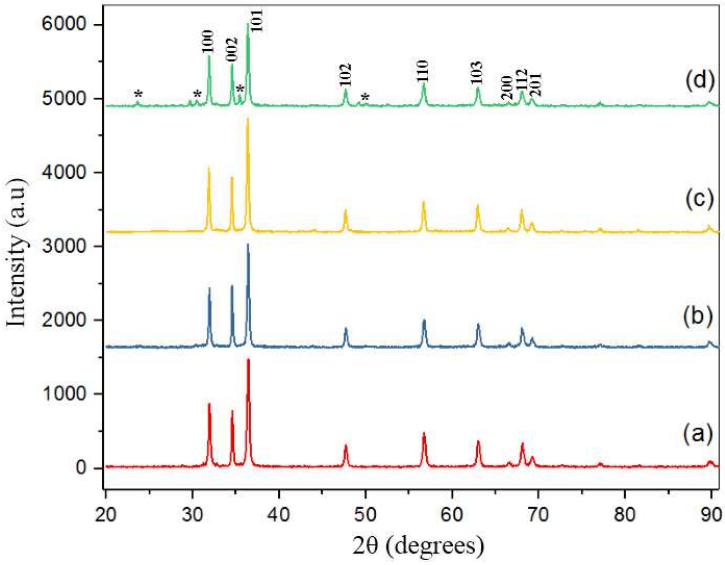

Fig. 2. XRD spectra of ZnO and ZnO:Cd nanostructures with a) 0%, b) 3%, c) 5% and d) 7% Cd.

Equation (1) (the Scherrer equation) was employed to calculate the mean crystallite size [24].

$$D = \frac{\lambda}{\beta \cos(\theta)} \quad (1)$$

, in which θ represents the Bragg diffraction angle, D the crystallite size, β the full width at half maximum and λ=1.5406 A˚ the wavelength of the incident radiation. The X-ray patterns showed reductions in the crystallite size of the Cd-doped samples from 44.48 to 37.14 nm with increasing the dopant concentration. The expansion of the unit cell caused by the replacement of Cd^{2+} ions exerted an internal strain on the growth of nanostructures and thus reduced the crystallite size [24, 30]. Equation (2) was utilized to derive the hexagonal lattice constants, i.e. a and c, of the ZnO:Cd and ZnO nanostructures [24].

$$\frac{1}{d^2} = \frac{4}{3}\left[\frac{h^2+hk+k^2}{a^2}\right] + \frac{l^2}{c^2} \quad (2)$$

, in which hkl represents Miller indices and d the distance between crystalline planes. Slight increases observed in the lattice constants with the Cd concentration can be explained by the larger radius of Cd^{2+} ions than that of Zn^{2+} ions (Table 1) [30].

Table 1: Lattice parameters and crystallite size of the ZnO and ZnO:Cd nanostructures.

Samples (%Cd)	a (Å)	c (Å)	c/a ratio	D (nm)
0%	3.238	5.194	1.6041	44.48
3%	3.239	5.195	1.6039	42.08
5%	3.239	5.198	1.6048	40.50
7%	3.242	5.199	1.6036	37.14

According to figure 3, FESEM was conducted on the ZnO nanostructures to explore the impact of the Cd dopant concentration on their morphology. The pure sample comprised nanorods and nanoparticles, and increases in the number and size of the nanorods with a rise in the Cd dopant concentration can be explained by the larger radius of Cd^{2+} (0.97 Å) than that of Zn^{2+} (0.74 Å).

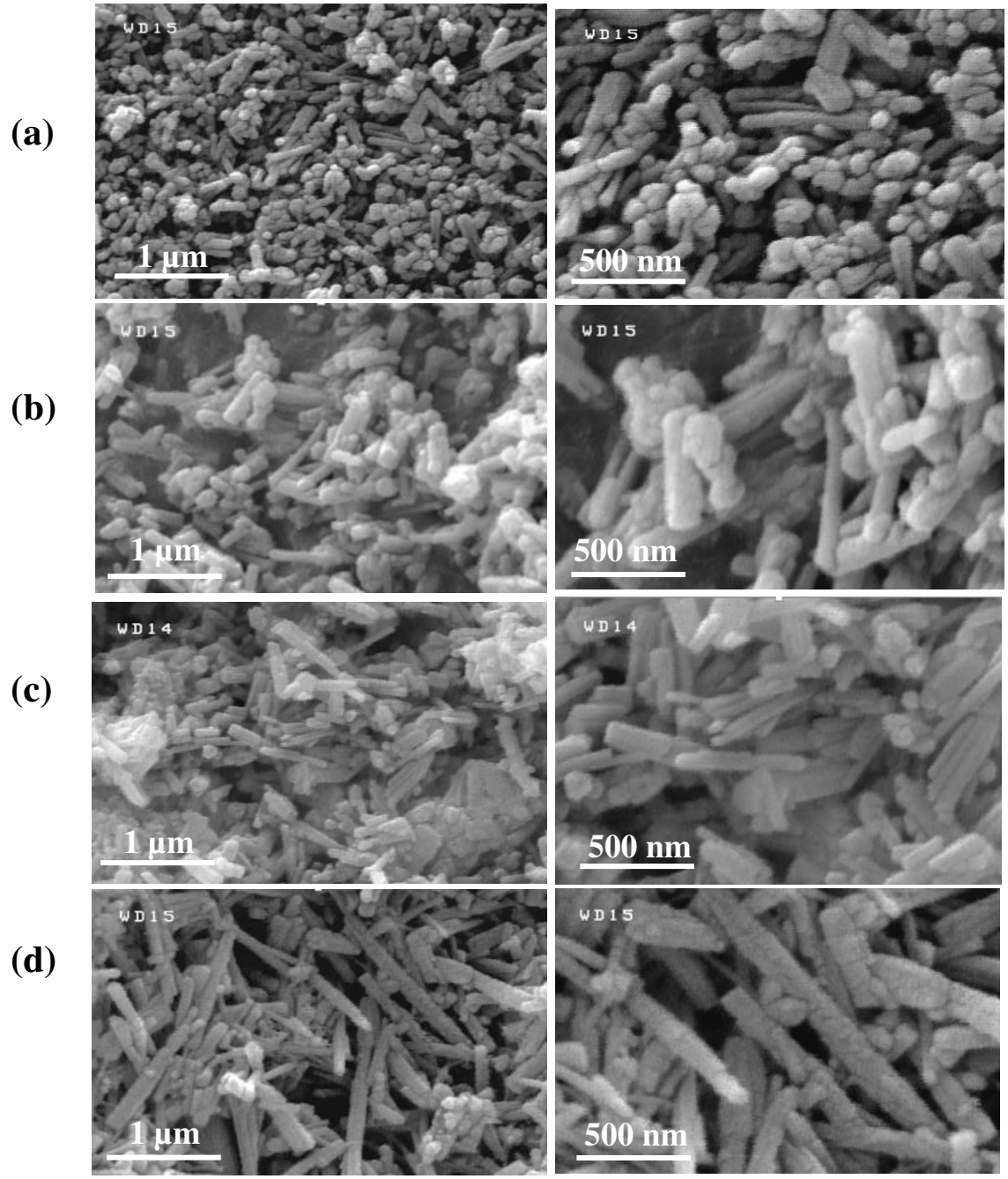

Fig. 3. FESEM images of the ZnO and ZnO:Cd nanostructures with a) 0%, b) 3%, c) 5% and d)7% Cd.

Table 2 presents the sizes of the nanostructures, suggesting that a rise in the doping levels of Cd increased the length of the nanorods. In addition, the morphological variations are explained by the fact that the Cd-O bond energy was lower than the bond energy of Zn-O, which caused differences between the polar and non-polar planes in terms of the surface energy, raised the vertical growth and prevented their sidelong growth [24]. Moreover, XRD and FESEM yielded consistent results.

Table 2: The length and diameter of the Cd-doped nanorods

Samples (%Cd)	Avg. Diameter (nm)	Avg. length (nm)
0%	50-60	300-400
3%	50-70	500-650
5%	40-60	600-700
7%	60-75	850 - 1000

3.2 Optical properties

Figure 4 illustrates the PL spectra of ZnO and ZnO:Cd, suggesting a sharp and highly-intense peak at 380 nm (3.26 eV) in the UV zone for all the samples, which were excited at room temperature and a wavelength of 325 nm. The recombination of excitons through an exciton-exciton collision process caused the emergence of an emission peak as large as the gap energy in the UV region. A second peak was observed in the so-called defect emission region at 430-600 nm. An increase in the Cd dopant concentration caused this defect emission to emerge, a phenomenon that is often reported in doped semiconductors [31].

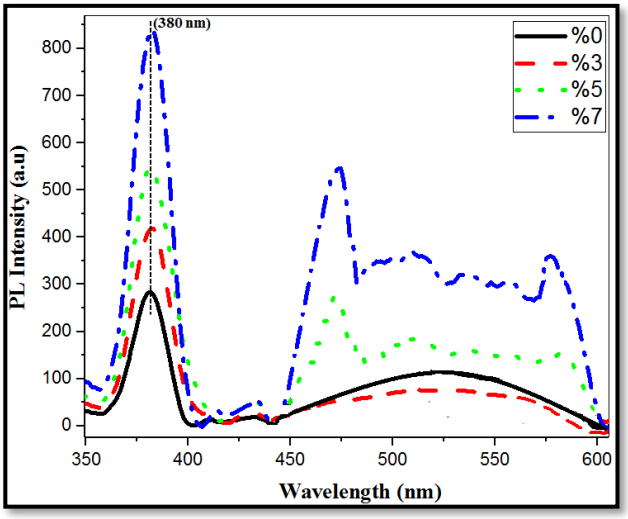

Fig. 4. PL spectra of ZnO and ZnO:Cd nanostructures (λ_{ex}=325 nm).

A rise in the Cd concentration to more than 3% substituted larger-size Cd^{2+} ions for Zn^{2+} ions, caused the emergence of peaks at 443, 474 and 583 nm, created crystallite stress and raised the number of defects, including Zn interstitials and oxygen vacancies [24].

The emission peak at 474 nm corresponds to structural defects of the product such as oxygen vacancies as the cause of visible green emissions [32, 33]. Emission peaks at 583 and 443 nm were respectively associated with the transition of oxygen vacancies and Zn interstitials [24]. The peaks were intensified as the Cd dopant concentration exceeded 3%, which also increased defects in the crystalline structure through developing surface defects, including Zn interstitials and oxygen vacancies. Doping therefore plays a key role in developing surface defects.

3.3 Electrical properties

Current-voltage specifications were obtained in the dark and under UV radiation at 350 nm, -10 to 10 V and 15.5 mW/cm^2 to examine the UV photodetectors based on ZnO:Cd nanostructures. The photocurrent versus the voltage followed the Schottky curve, suggesting a Schottky contact between the nanostructures and the aluminum electrode. Although the dark current through the samples was as low as 0.29, 0.35, 0.42 and 0.50 nA at various Cd concentration, it increased in all the samples under UV radiation. The photocurrent of the samples ($I_{illuminated} - I_{dark}$) was derived as 32.08, 162.15, 320.21 and 460.10 nA. The XRD results suggested variations in the growth direction of the ZnO:Cd nanostructures increased the photocurrent through the doped samples [34]. The I-V curve of the samples are compared in figure 5, showing the higher photocurrent of the Cd-doped samples than that of the pure sample. The superiority of the illumination current over the dark current indicates the sensitivity of the present study structures to UV radiation, which should be therefore used in UV photodetectors. The photocurrent increased to its maximum with an increase in Cd levels to 7%.

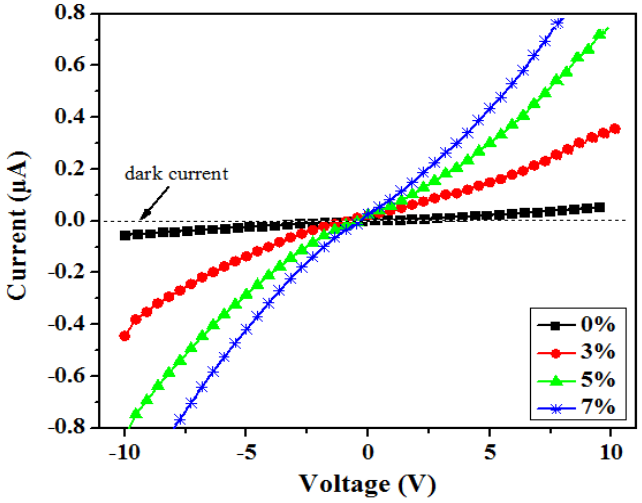

Fig. 5. The I-V specifications of ZnO and ZnO:Cd nanostructures for different Cd concentration from −10 V to 10 V.

Doping ZnO with Cd enhances its electrical conductivity through raising carrier concentrations in its structure [26]. Replacing Zn^{2+} with Cd^{2+} increased defects in the donor, which improved the n-type carrier concentration of ZnO and created more Zn interstitials and oxygen vacancies [24]. Increases in V_O, i.e. oxygen vacancy, and n-type properties of the Zn-Cd-V_O complex, with a low ionization and formation energy, increased

carrier concentrations and conductivity [26]. Figure 4 shows the results of the PL analysis, which confirm these findings. In addition, incorporating Cd into ZnO raises the numbers of Cd interstitial and substitutional and sites as donors [26]. Increases in the number of donor defects therefore increase the number of oxygen molecules adsorbed on the nanostructure surface in the dark. UV radiation increases the number of holes trapped by oxygen ions and causes more free electrons to contribute to producing the photocurrent.
Table 2 shows the higest photocurrent in the longest sample doped with 7% Cd. According to the UV photodetection mechanism, increasing the length of nanorods raise the number of oxygen molecules adsorbed on their surface in the dark. UV radiation therefore increases the number of holes in which oxygen ions are trapped and also the photocurrent produced through increasing the number of free electrons [35-36].
Photodetectors can be appraised using parameters such as detectivity (D*) and responsivity (R), which are obtained using equations (3)-(4) [37].

$$R = \frac{I_{ph}}{P_{inc}} \tag{3}$$

$$D^* = \frac{R}{(2eI_{dark})^{1/2}} \tag{4}$$

, in which I_{dark} represents the dark current, e the unit charge, I_{ph} the photocurrent and P_{inc} the incident optical power. Table 3 summarizes the detectivity and responsivity of the ZnO and ZnO:Cd nanostructures at 5 V.
Figure 6 shows the ratio of the photocurrent to dark current (I_{ph}/I_{dark}) as the sensitivity of the photodetectors, suggesting a sensitivity of 110.62, 463.28, 762.40 and 920.30 for the ZnO and ZnO:Cd photodetectors, respectively. The higher sensitivity observed in the samples doped with Cd compared to in pure ZnO can be explained by increases in the illumination current in the ZnO:Cd samples.

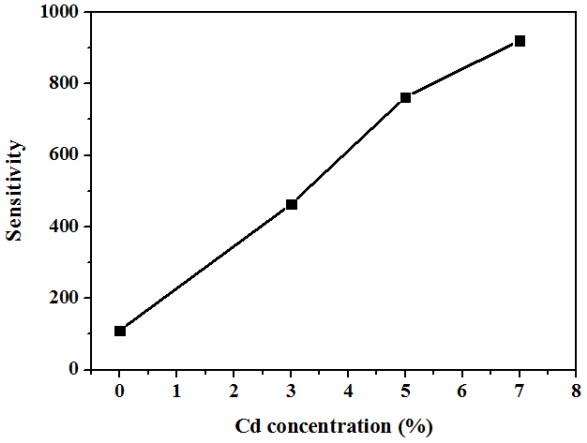

Fig. 6. Sensitivity of ZnO and ZnO: Cd nanostructures as a function of Cd concentration.

Response time is also used for the qualitative measurement of UV photodetectors. Figure 7 shows temporal variations in the photoresponse of the samples under UV radiation at 350 nm, 15.5 mW/cm^2 and a 5 V on-off bias. The layers underwent a cycle twice; i.e. they were exposed to UV radiation for three minutes and then placed in the dark for three minutes.

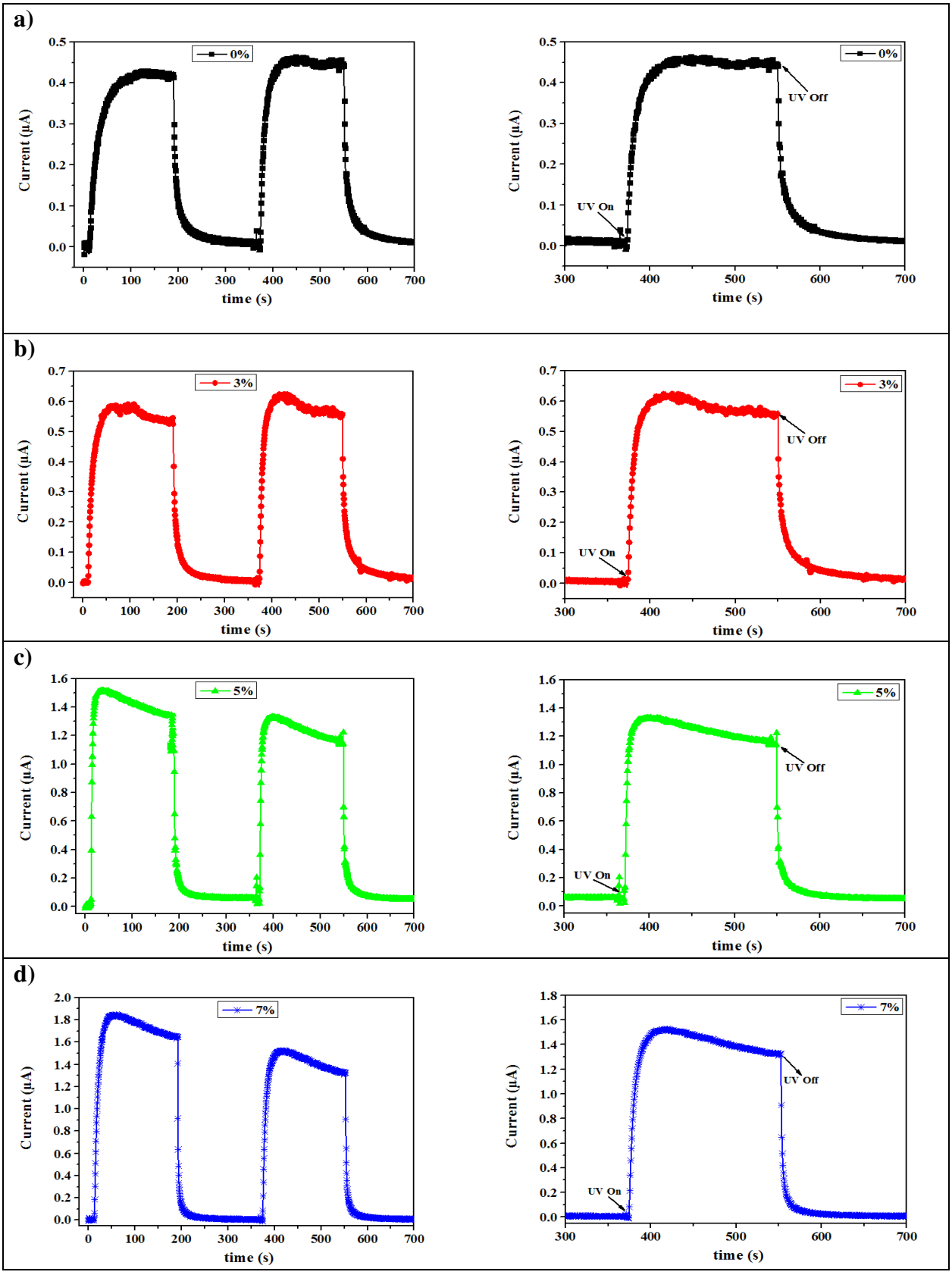
a)
0%
Current (μA)
time (s)
UV On
UV Off
b)
3%
c)
5%
d)
7%

Fig. 7. The I-t specification of the ZnO and ZnO:Cd nanostructures at different Cd concentrations (a) 0%, b) 3%, c) 5% and d) 7% measured with and without UV light illumination at 5 V.

This study observed the fast reversibility of the photodetectors and their appropriate repeatability. Under UV radiation, the current rapidly increased to a certain level and then returned to its original state as the lamp was turned off. Oxygen molecules were released under UV radiation through combining the holes generated by oxygen ions and adsorbed on the detector's surface. As discussed earlier, free electrons were trapped by oxygen molecules as UV lamp was turned off and oxygen molecules were re-adsorbed on the surface [35, 36]. UV radiation should be kept off for long enough to help the current through the detector return to its initial level and oxygen ions are completely adsorbed on its surface.

The rise time and decay time of a detector are respectively defined as the length of interval during which its current increases from 10% to 90% of its peak and decreases from 90% to 10% [38]. The following exponential equations are used to explain turn-on and turn-off as the transient response of the photodetectors [38]:

Turn on: $I(t) = I_0(t)\left[1 - \exp(\frac{-t}{\tau_r})\right]\beta$ (3)

Turn off: $I(t) = I_0(t)\left[1 - \exp(\frac{-t}{\tau_d})\right]\beta$ (4)

, in which τ, β, $I_0(t)$ and t respectively denote the time constant, the decay exponent, the transient current and the time passed after on/off. Furthermore, β was estimated at 1 using the fitted exponential formula, and τ_r=2.5 s was obtained as the rise time of the 5% Cd samples for turn-on and τ_d=4 s as the decay time of the 5% Cd samples for turn-off. The 5% Cd samples were therefore found to be excellent in terms of their photoresponse.

According to the FESEM results, incorporating Cd as a dopant changed the shape of the nanostructures from spherical to rod-shaped. Using one-dimensional ZnO:Cd nanostructures increased the surface effects by increasing the ratio of the surface area to the volume. The rates of absorbing and desorbing oxygen molecules on the surface of the nanostructures and the response of the photodetectors were therefore increased [11, 36]. Decreases in the diameter of ZnO:Cd nanorods were found to narrow the conduction channel of charge carriers (electrons), which were closer to the surface effects, which precipitated the re-absorption of oxygen molecules on the surface and increased the photoresponse speed of the detector [36]. The photoresponse of the 5% Cd nanorods with a relatively smaller diameter was also faster.

Table 3 presents the sensitivity, responsivity, photocurrent, decay time, rise time and detectivity of the photodetectors.

Table 3. The sensitivity, responsivity, photocurrent, decay time, rise time and detectivity of the ZnO and ZnO:Cd nanostructures measured at 5 V.

Samples (%Cd)	Photocurrent (nA)	Rise time (s)	Decay time (s)	Sensitivity (I_{ph}/I_d)	Responsivity (μA/W)	Detectivity (jones)
0%	32.08	18	13	110.62	2.07	0.22×10^9
3%	162.15	8	10	463.28	10.46	0.98×10^9

5%	320.21	2.5	4	762.40	20.66	1.8×10^9
7%	460.10	5	6	920.30	29.68	2.4×10^9

Figure 8 illustrates a model of the mechanism of charge transport in the MSM photodetectors based on ZnO:Cd nanorods. The adsorption of oxygen molecules (O_2) onto the surface of ZnO as negatively charged ions through capturing free electrons from the n-type ZnO structure can generate a low-conductivity depletion layer near the surface of pure ZnO nanorods in the dark $[O_2(\text{gas}) + e^- \rightarrow O_2^-(\text{adsorption})]$. Moreover, UV radiation (hv>Eg) photogenerates electron-hole pairs and discharges the adsorbed oxygen (O_2^-) ions through surface electron-hole recombination on the pure ZnO nanorods $[h\nu \rightarrow e^- + h^+]$. The electrons of the pair remaining in the conduction band increase conductivity $[O_2^-(\text{adsorption}) + h^+ \rightarrow O_2(\text{gas})]$. In contrast, the arrays of the ZnO:Cd nanorods with a large surface-to-volume ratio can cause their adsorption onto and desorption from the surface of ZnO:Cd [19, 24]. Their response rate and carrier concentration in the ZnO:Cd structure can be therefore significantly improved; they can further contribute to increasing the number of oxygen vacancies generated, which improves the photocurrent of ZnO:Cd photodetectors. Zn^{2+} ions in the ZnO lattice can be easily replaced by Cd^{2+} ions. The positive charge of the substituted Zn^{2+} site (formation of electron-donor defects [Cd_{Zn}]) should be, however, compensated through releasing electrons to keep its electrical neutrality. Cd-doping inroduces electrons into the conduction band of the sample and therefore increases the concentration of free electrons and lower the resistivity of the ZnO:Cd material, which thus increases responsivity. According to Figure 8 and the trapping mechanism of oxygen adsorption/desorption, ZnO:Cd nanorods are thoroughly recommended for UV detection.

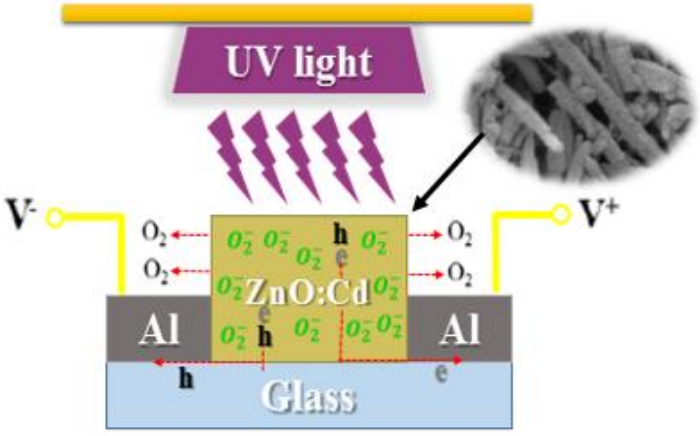

Figure 8. Schematic diagram of the ZnO:Cd nanorod photodetectors under UV radiation.

Table 4 compares the results of doping ZnO with different materials in photodetectors, suggesting improvements in the characteristics of UV photodetectors through doping the ZnO structure with Cd. This device is therefore applicable to UV photodetection.

Table 4: Comparing the results of UV photodetection between this study and recent reports.

Device structure	Bias (V)	Rise time (s)	Decay time (s)	Sensitivity (I_{ph}/I_d)	References
Fe-ZnO	1	21.2	24.7	<10	39

Ga-ZnO	1	29.75	89.67	11.07	40
3 at% Cd-ZnO	5	37.03	221.93	93.78	41
10 at% Mg-ZnO	5	94	89.6	71.68	42
4 at% Ni-ZnO	3	70	43	393.04	17
3 at% Cu-ZnO	3	58	83	192.6	18
Fe-ZnO	3	46	37	471.1	19
ZnO: Cd (5%)	5	2.5	4	762.40	Present
ZnO: Cd (7%)	5	5	6	920.30	Present

4. Conclusion

The present study performed thermal decomposition as a simple, fast and cost-effective technique to synthesize ZnO and ZnO nanostructures doped with 3, 5 and 7% Cd. The XRD patterns showed the hexagonal wurtzite structure of the study samples and that (002) plane to be the preferred orientation in the nanostructures. According to the results of FESEM, variations in the Cd concentration can morphologically influence the ZnO nanostructures. UV photodetectors were fabricated by employing the synthesized ZnO:Cd structures. Developing ZnO UV photodetectors faces challenges such as photocurrent saturation and fast relaxation. The rise-decay time of the UV photodetectors based on ZnO:Cd (5%) was lower than that of pure ZnO and their sensitivity was excellent under UV radiation. In other words, the photoresponse and sensitivity of the doped samples were maximized.

References

[1] Y. Kim, S. J. Kim, S. P. Cho, B. H. Hong, D. J. Jang, High-performance UV PDs based on solution-grown ZnS nanobelts sandwiched between graphene layers, Scientific reports, 5 (2015) 12345. https://doi.org/10.1038/srep12345.

[2] A. Sciuto, A. Meli, L. Calcagno, S. Di Franco, M. Mazzillo, G. Franzo, S. Albergo, A. Tricomi, D. Longo, G. Giudice, G. D'Arrigo, Large-area SiC-UV photodiode for spectroscopy portable system, IEEE Sensors Journal, 19 (2019) 2931-2936. https://doi.org/10.1109/JSEN.2019.2891833.

[3] T. J. Chang, T. J. Hsueh, A NO2 Gas Sensor with a TiO2 Nanoparticles/ZnO/MEMS-Structure that is Produced Using Ultrasonic Wave Grinding Technology, Journal of The Electrochemical Society 167 (2020) 027521. https://doi.org/10.1149/1945-7111/ab69f0.

[4] S. J. Young, T. H. Wang, ZnO nanorods adsorbed with photochemical Ag nanoparticles for IOT and field electron emission application, ournal of The Electrochemical Society, 165 (2018) B3043. https://doi.org/10.1149/2.0061808jes.

[5] L. W. Ji, S. M. Peng, Y. K. Su, S. J. Young, C. Z. Wu, W. B. Cheng, UV PDs based on selectively grown ZnO nanorod arrays, Applied Physics Letters, 94 (2009) 203106. https://doi.org/10.1063/1.3141447.

[6] M. Boujnah, M. Boumdyan, S. Naji, A. Benyoussef, A. El Kenz, M. Loulidi, High efficiency of transmittance and electrical conductivity of V doped ZnO used in solar cells applications, Journal of Alloys and Compounds, 671 (2016) 560-565. https://doi.org/10.1016/j.jallcom.2016.02.107.

[7] Y.J. Park, H. Song, K.B. Ko, B.D. Ryu, T.V. Cuong, C.H. Hong, Nanostructural effect of ZnO on light extraction efficiency of near-ultraviolet light-emitting diodes, Journal of Nanomaterials, 2016 (2016) 1-6. https://doi.org/10.1155/2016/7947623.
[8] S.K. Singh, P. Hazra, S. Tripathi, P. Chakrabarti, Performance analysis of RF-sputtered ZnO/Si heterojunction UV photodetectors with high photoresponsivity, Superlattices and Microstructures, 91 (2016) 62-69. https://doi.org/10.1016/j.spmi.2015.12.036.
[9] S. J. Young, Y. H. Liu, High response of ultraviolet photodetector based on Al-doped ZnO nanosheet structures, IEEE Journal of Selected Topics in Quantum Electronics, 23 (2017) 1-5. https://doi.org/10.1109/JSTQE.2017.2684540.
[10] M. Zare, S. Safa, R. Azimirad, S. Mokhtari, Graphene oxide incorporated ZnO nanostructures as a powerful ultraviolet composite detector, Materials Science: Materials in Electronics, 28 (2017) 6919-6927. https://doi.org/10.1007/s10854-017-6392-x.
[11] R. Shabannia, High-sensitivity UV photodetector based on oblique and vertical Co-doped ZnO nanorods, Materials Letters, 214 (2018) 254-256. https://doi.org/10.1016/j.matlet.2017.12.019.
[12] Y. Zhang, E. W. Shi, Z. Z. Chen, Magnetic properties of different temperature treated Co-and Ni-doped ZnO hollow nanospheres, Materials science in semiconductor processing, 13 (2010) 132-136. https://doi.org/10.1016/j.mssp.2010.05.002.
[13] C.C. Vidyasagar, Y. Arthoba Naik, T.G. Venkatesh, R. Viswanatha, Solid-state synthesis and effect of temperature on optical properties of Cu–ZnO, Cu–CdO and CuO nanoparticles, Powder technology, 214 (2011) 337-343. https://doi.org/10.1016/j.powtec.2011.08.025.
[14] S. Safa, S. Mokhtari, A. Khayatian, R. Azimirad, Improving ultraviolet photodetection of ZnO nanorods by Cr doped ZnO encapsulation process, Optics Communications, 413 (2018) 131-135. https://doi.org/10.1016/j.optcom.2017.12.038.
[15] F. Li, C. Zhu, S. Ma, A. Sun, H. Song, X. Li, X. Wang, Investigation of the blue–green emission and UV photosensitivity of Cu-doped ZnO films, Materials science in semiconductor processing, 16 (2013) 1079–1085. https://doi.org/10.1016/j.mssp.2013.03.012.
[16] R. Rajalakshmi, S. Angappane, Synthesis, characterization and photoresponse study of undoped and transition metal (Co, Ni, Mn) doped ZnO thin films, Materials Science and Engineering: B, 178 (2013) 1068–1075. https://doi.org/10.1016/j.mseb.2013.06.015.
[17] Y. L. Chu, L. W. Ji, Y. J. Hsiao, H. Y. Lu, S. J. Young, I. T. Tang, T. T. Chu, X. J. Chen, Fabrication and Characterization of Ni-Doped ZnO Nanorod Arrays for UV Photodetector Application, Journal of The Electrochemical Society, 167 (2020) 067506. https://doi.org/10.1149/1945-7111/ab7d43.
[18] Y. L. Chu, L. W. Ji, H. Y. Lu, S. J. Young, I. T. Tang, T. T. Chu, J. S. Guo, Y. T. Tsai, Fabrication and Characterization of UV Photodetectors with Cu-Doped ZnO Nanorod Arrays, Journal of The Electrochemical Society, 167 (2020), 027522. https://doi.org/10.1149/1945-7111/ab69f2.
[19] Y. L. Chu, S. J. Young, L. W. Ji, I. T. Tang, T. T. Chu, Fabrication of Ultraviolet Photodetectors Based on Fe-Doped ZnO Nanorod Structures, Sensors, 20 (2020), 3861. https://doi.org/10.3390/s20143861.
[20] R. Anitha, R. Ramesh, R. Loganathan, D. S. Vavilapalli, K. Baskar, S. Singh, Large area ultraviolet photodetector on surface modified Si: GaN layers, Applied Surface Science, 435 (2018) 1057-1064. https://doi.org/10.1016/j.apsusc.2017.11.097.
[21] S. I. Inamdar, V. V. Ganbavle, and K. Y. Rajpure, ZnO based visible–blind UV photodetector by spray pyrolysis, Superlattices and Microstructures, 76 (2014) 253-263. https://doi.org/10.1016/j.spmi.2014.09.041.
[22] R. Bahramian, H. Eshghi, A. Moshaii, Influence of annealing temperature on morphological, optical and UV detection properties of ZnO nanowires grown by chemical bath deposition, Materials & Design, 107 (2016) 269-276. https://doi.org/10.1016/j.matdes.2016.06.047.
[23] S. Vijayalakshmi, S. Venkataraj, R. Jayavel, Characterization of cadmium doped zinc oxide (Cd : ZnO) thin films prepared by spray pyrolysis method, Journal of Physics D: Applied Physics, 41 (2008) 245403. https://doi.org/10.1088/0022-3727/41/24/245403.

[24] Y. Purusothaman, N. Rao Alluri, A. Chandrasekhar, S. J. Kim, Elucidation of the unsymmetrical effect on the piezoelectric and semiconducting properties of Cd-doped 1D-ZnO nanorods, Journal of Materials Chemistry C, 5 (2017) 415-426. https://doi.org/10.1039/c6tc04592h.
[25] L. T. Jule, F. B. Dejene, A. G. Ali, K. T. Roro, A. Hegazy,N. K. Allam, E. E. Shenawy, Wide visible emission and narrowing band gap in Cd-ZnO:Cd nanopowders synthesized via a sol-gel route, Journal of Alloys and Compounds, 687 (2016) 920-926. https://doi.org/10.1016/j.jallcom.2016.06.176.
[26] J. Y. Kim, J. Kim, J. Roh, H. Kim, C. Lee, Efficiency Improvement of Organic Photovoltaics Adopting Li-and Cd-ZnO:Cd Electron Extraction Layers, IEEE Journal of Photovoltaics, 6 (2016) 930-933. https://doi.org/10.1109/JPHOTOV.2016.2553780.
[27] B. Madavali, H. S. Kim, S. J. Hong, Thermally decomposition of high-quality flower-like ZnO nanorods from zinc acetate dehydrate, Materials Letters, 132 (2014) 342-345. https://doi.org/10.1016/j.matlet.2014.06.111.
[28] C. C. Lin, Y. Y. Li,Synthesis of ZnO nanowires by thermal decomposition of zinc acetate dihydrate, Journal of Materials Chemistry and Physics, 113 (2009) 334-337. https://doi.org/10.1016/j.matchemphys.2008.07.070.
[29] F. Abbasi, F. Zahedi, M. hasan Yousefi, Fabricating and investigating high photoresponse UV photodetector based on Ni-doped ZnO nanostructures, Journal of Optics Communications, 482 (2020) 126565. https://doi.org/10.1016/j.optcom.2020.126565.
[30] R. Saravanan, F. Gracia, M. M. Khan,V. Poornima, V. K. Gupta,V. Narayanan,A. Stephen, ZnO/CdO nanocomposites for textile effluent degradation and electrochemical detection, Journal of Molecular Liquids, 209 (2015) 374-380. https://doi.org/10.1016/j.molliq.2015.05.040.
[31] S. M. Shah, H. Naz, R. N. Ali, F. Alam, A. Ali, M. Farooq, A. Shah, A. Badshah, M. Siddiq, A. Waseem, Optical and morphological studies of transition metal doped ZnO nanorods and their applications in hybrid bulk heterojunction solar cells, Arabian journal of chemistry, 10 (2017) 1118-1124. https://doi.org/10.1016/j.arabjc.2014.10.001.
[32] M. Debbichia, M. Souissi, A. Fouzri, G. Schmerber, M. Said, M. Alouani, Room temperature ferromagnetism in Cd-doped ZnO thin films through defect engineering, Journal of Alloys and Compounds, 598 (2014) 120-125. https://doi.org/10.1016/j.jallcom.2014.01.247.
[33] Y. Peng, S. Qin, W. S. Wangb, A. W. Xu, Fabrication of porous Cd-doped ZnO nanorods with enhanced photocatalytic activity and stability, CrystEngComm, 15 (2013) 6518-6525. https://doi.org/10.1039/C3CE40798E.
[34] V. S. Bhati, S. Ranwa, M. Fanetti, M. Valant, M. Kumar, Efficient hydrogen sensor based on Ni-doped ZnO nanostructures by RF sputtering, Sensors and Actuators B: Chemical, 255 (2018) 588-597. https://doi.org/10.1016/j.snb.2017.08.106.
[35] L. Guoa, H. Zhang, D. Zhao, B. Li, Z. Zhang, M. Jiang, D. Shen, High responsivity ZnO nanowires based UV detector fabricated by the dielectrophoresis method, Sensors and Actuators B:Chemical, 166 (2012) 12-16. https://doi.org/10.1016/j.snb.2011.08.049.
[36] Q. Zhu, C. Xie, H. Li, D. Zeng, A method for modeling and deciphering the persistent photoconductance and long-term charge storage of ZnO nanorod arrays, Nano Research, 9 (2016) 2972-3002. https://doi.org/10.1007/s12274-016-1182-y.
[37] X. Yu, H. N. Tsao, Z. Zhang, P. Gao, Miscellaneous and Perspicacious: Hybrid Halide Perovskite Materials Based Photodetectors and Sensors, Journal of Advanced Optical Materials, (2020) 2001095. https://doi.org/10.1002/adom.202001095.
[38] S. Safa, S. Mokhtari, A. Khayatian, R. Azimirad, Improving ultraviolet photodetection of ZnO nanorods by Cr doped ZnO encapsulation process, Optics Communications, 413 (2018) 131-135. https://doi.org/10.1016/j.optcom.2017.12.038.
[39] S. J. Chang, C. W. Liu, C. H. Hsiao, K. Y. Lo, S. J. Young, T. H. Kao, K. S. Tsai, S. L. Wu, Noise properties of Fe-ZnO nanorod ultraviolet photodetectors, IEEE Photonics Technology Letters, 25 (2013) 2089-2092. https://doi.org/10.1109/LPT.2013.2281467.

[40] C. H. Hsiao, C. S. Huang, S. J. Young, S. J. Chang, J. J. Guo, C. W. Liu, T. Y. Yang, Field-emission and photoelectrical characteristics of Ga–ZnO nanorods photodetector, IEEE transactions on electron devices, 60 (2013) 1905-1910. https://doi.org/10.1109/TED.2013.2257790.
[41] N. Kumar, A. Srivastava, Faster photoresponse, enhanced photosensitivity and photoluminescence in nanocrystalline ZnO films suitably doped by Cd, Journal of Alloys and Compounds, 706 (2017) 438-446. https://doi.org/10.1016/j.jallcom.2017.02.244.
[42] N. Kumar, A. Srivastava, Green photoluminescence and photoconductivity from screen-printed Mg doped ZnO films, Journal of Alloys and Compounds, 735 (2018) 312-318. https://doi.org/10.1016/j.jallcom.2017.11.024.

Figures

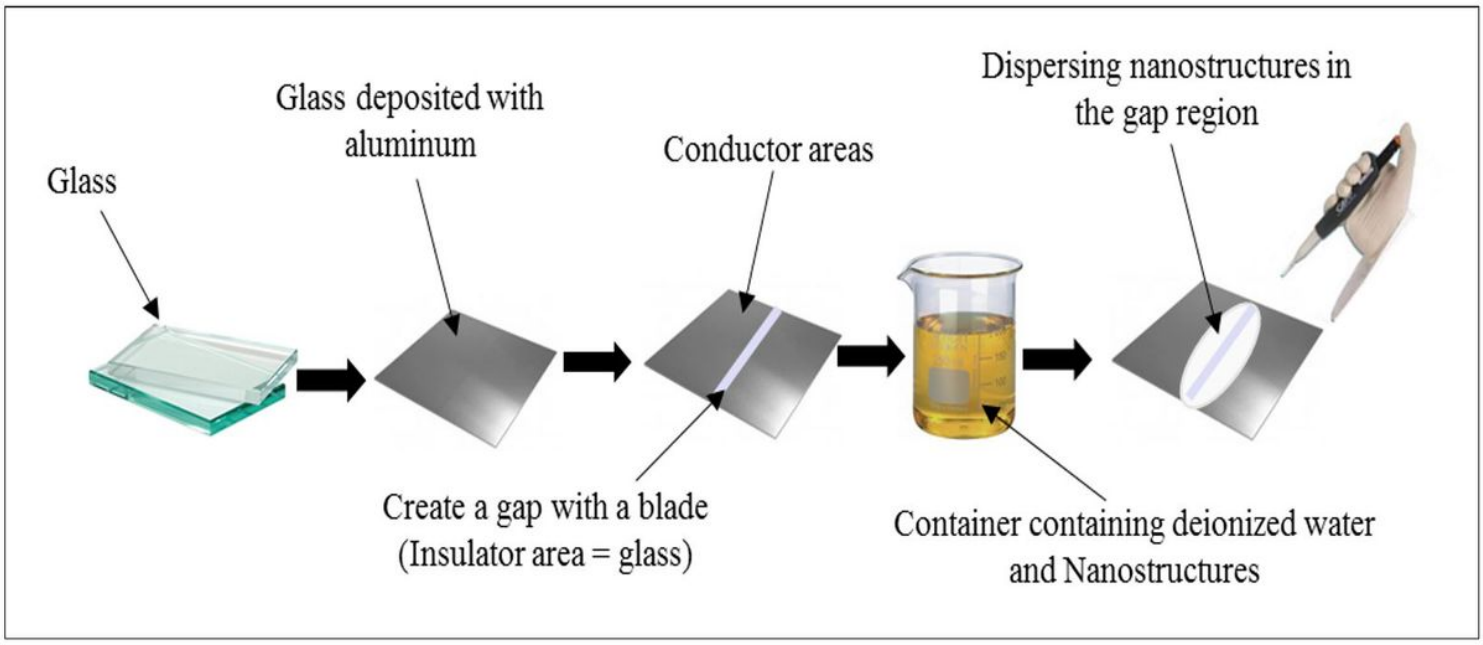

Figure 1

Schematic structure of the UV photodetector [29].

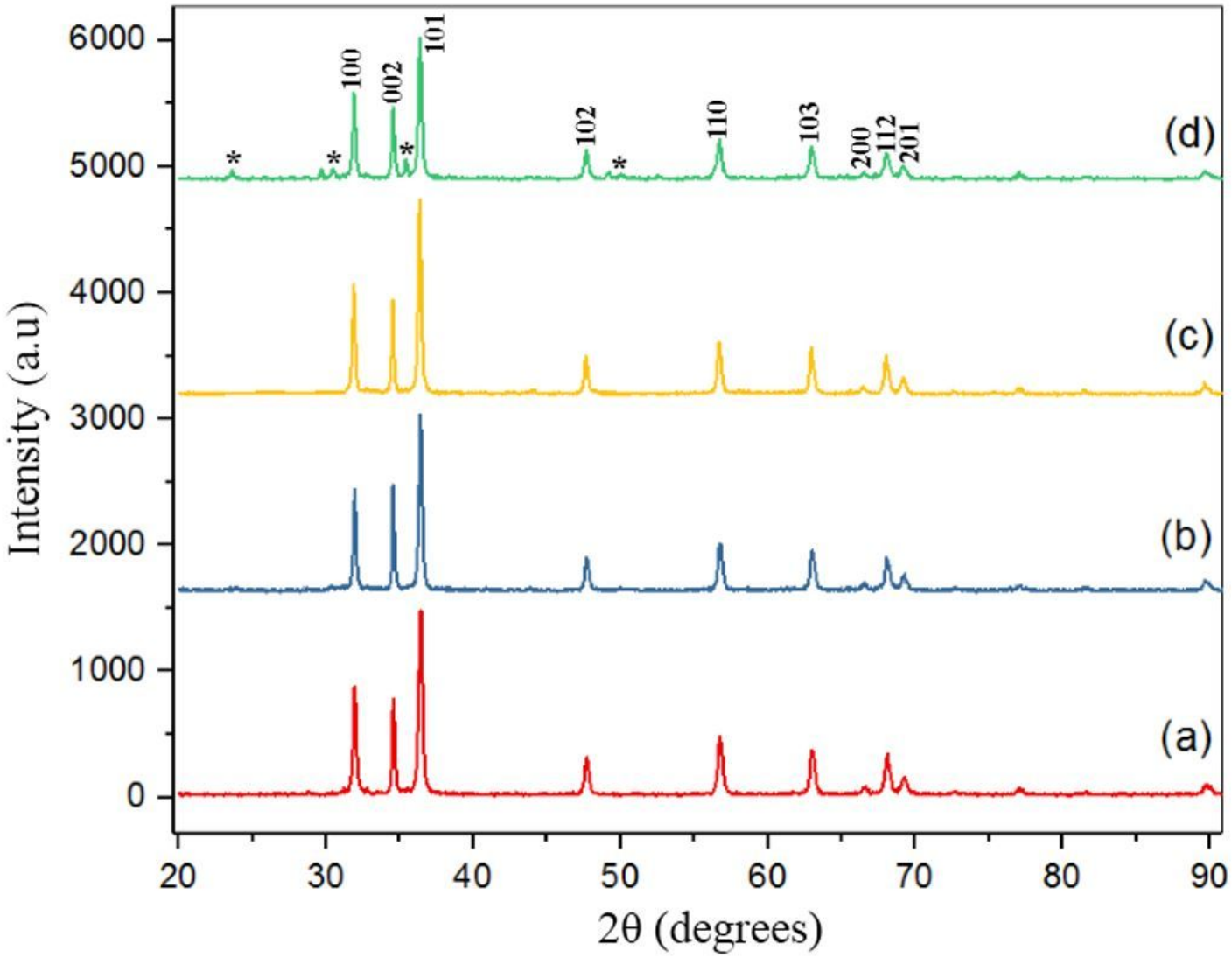

Figure 2

XRD spectra of ZnO and ZnO:Cd nanostructures with a) 0%, b) 3%, c) 5% and d) 7% Cd. Equation (1) (the Scherrer equation) was employed to calculate the mean crystallite size [24].

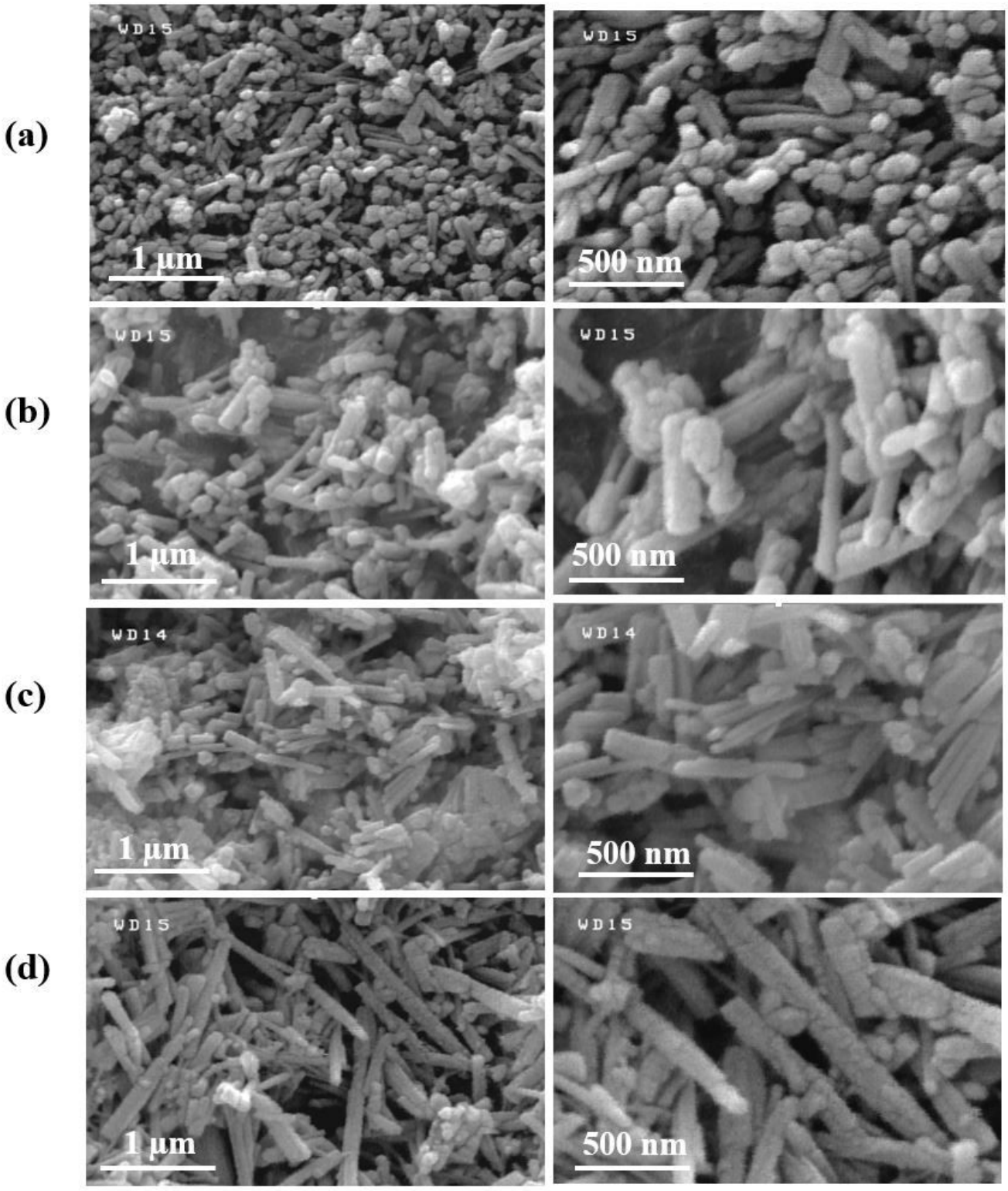

Figure 3

FESEM images of the ZnO and ZnO:Cd nanostructures with a) 0%, b) 3%, c) 5% and d)7% Cd.

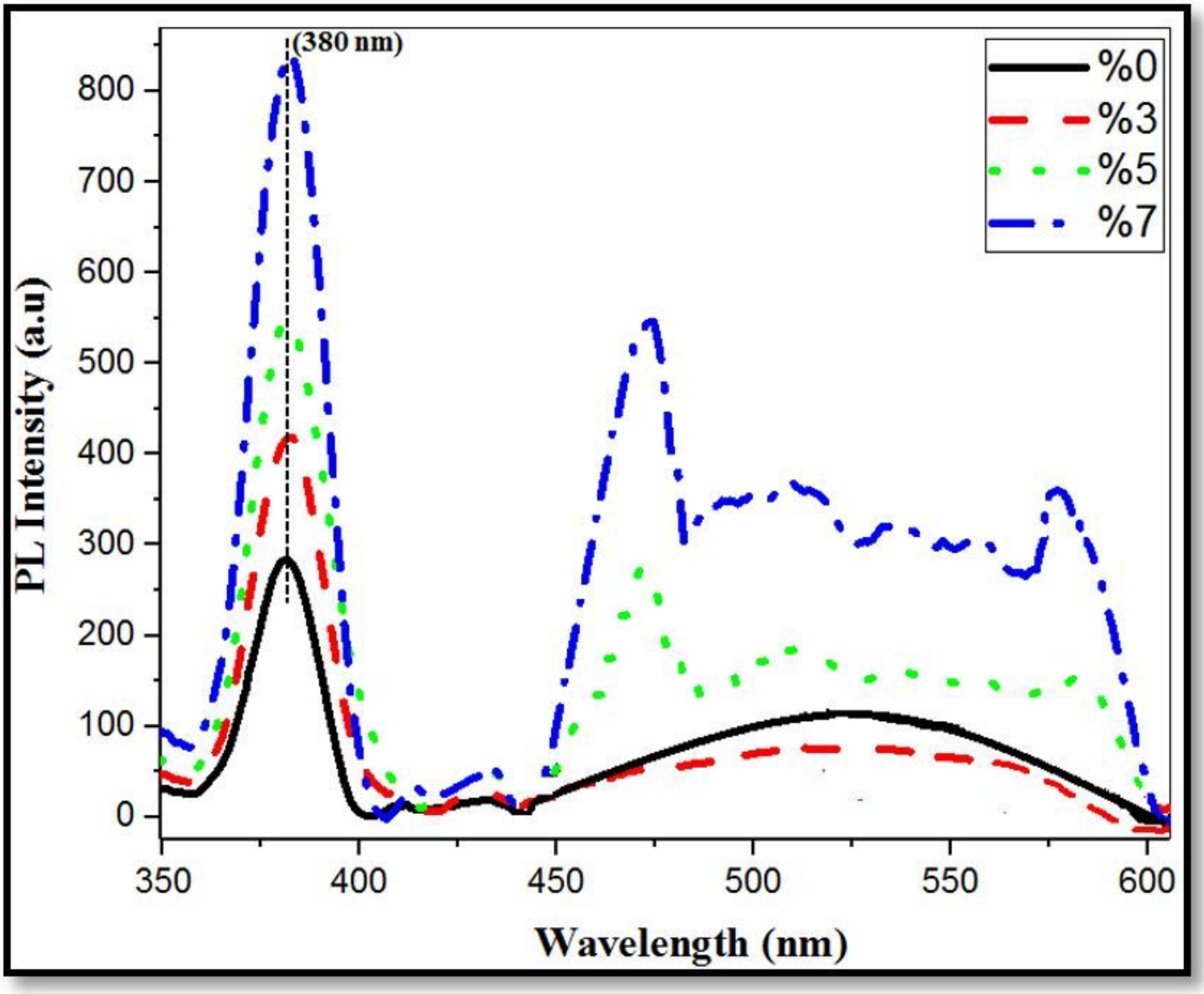

Figure 4

PL spectra of ZnO and ZnO:Cd nanostructures (λex +325 nm).

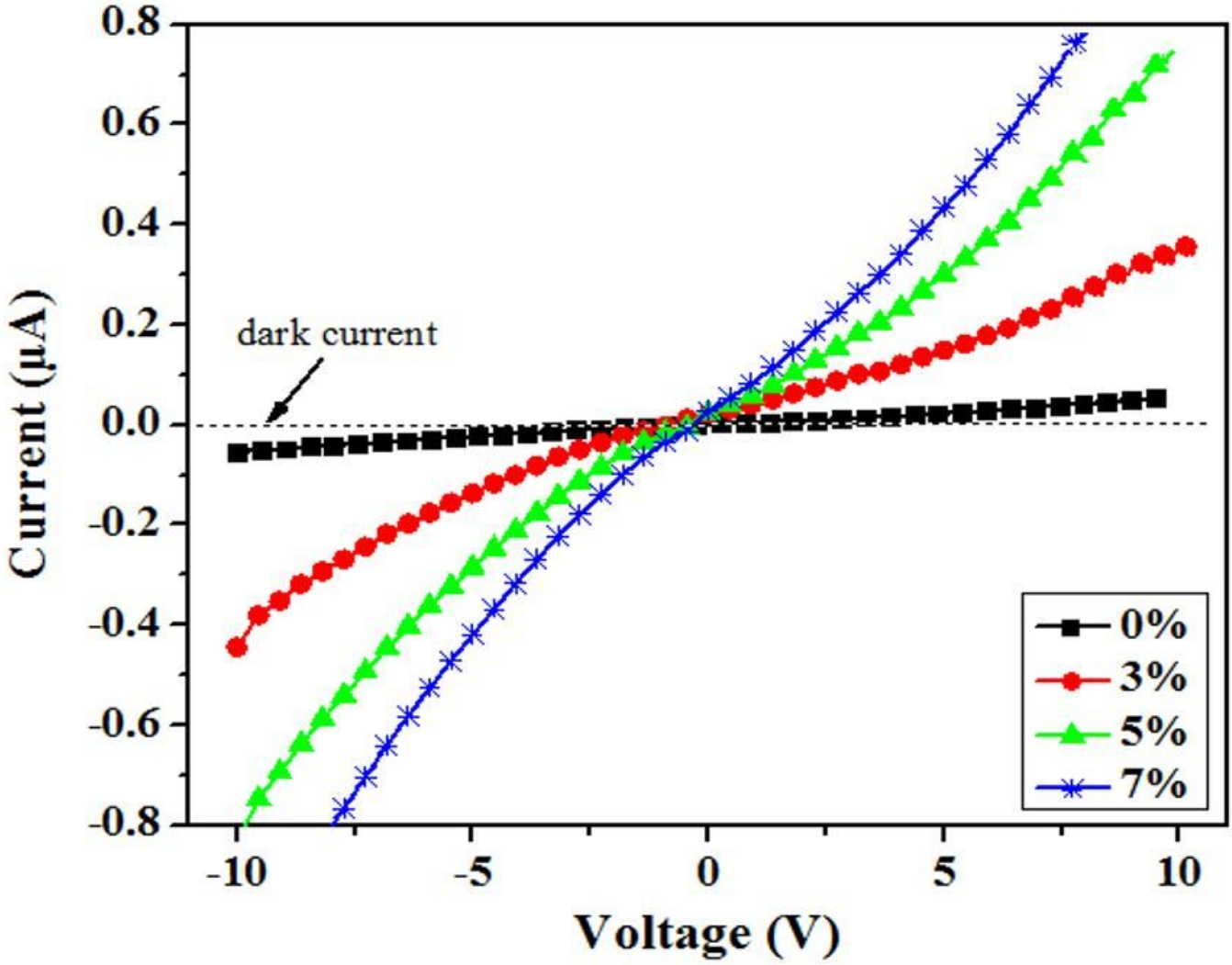

Figure 5

The I-V specifications of ZnO and ZnO:Cd nanostructures for different Cd concentration from −10 V to 10 V.

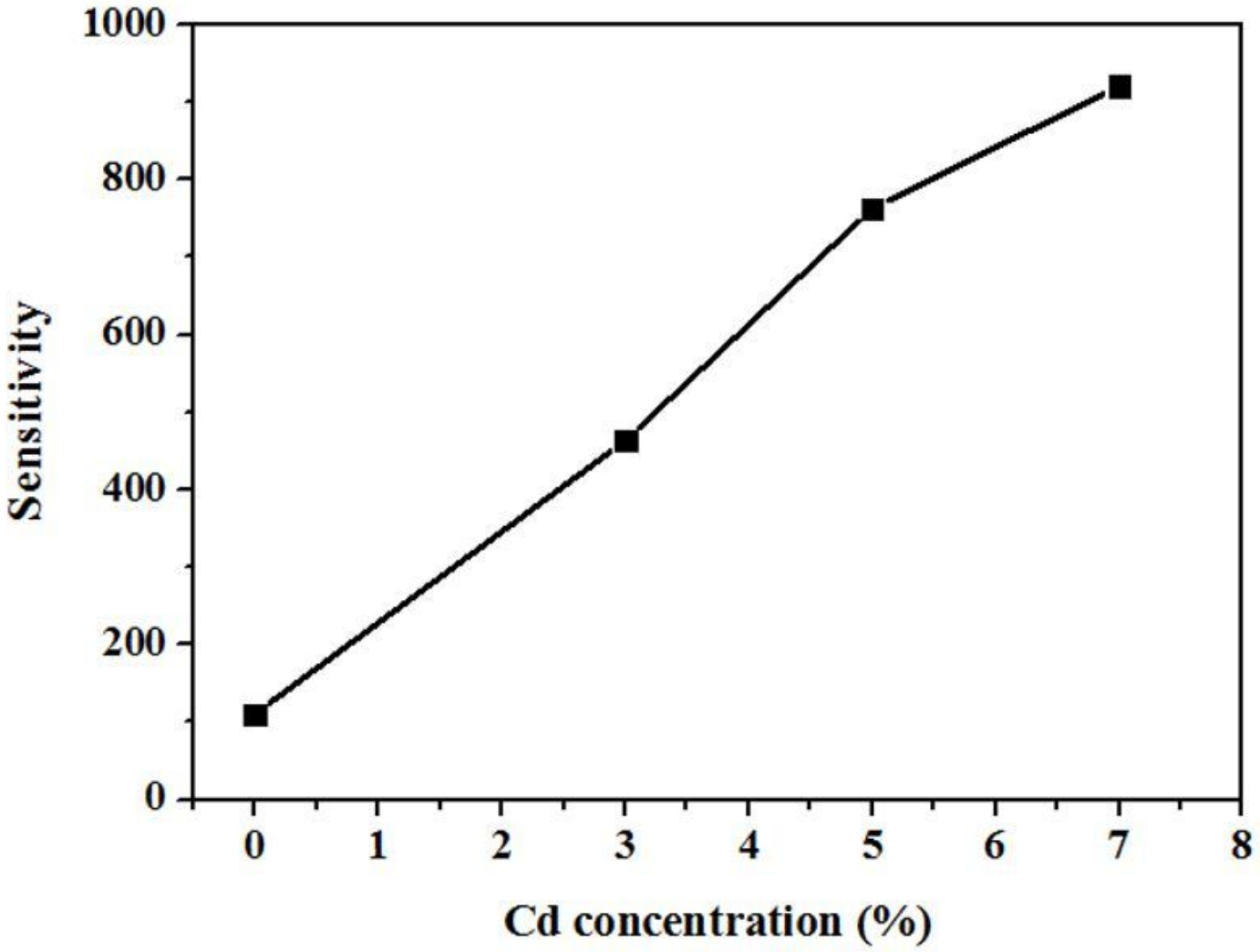

Figure 6

Sensitivity of ZnO and ZnO: Cd nanostructures as a function of Cd concentration.

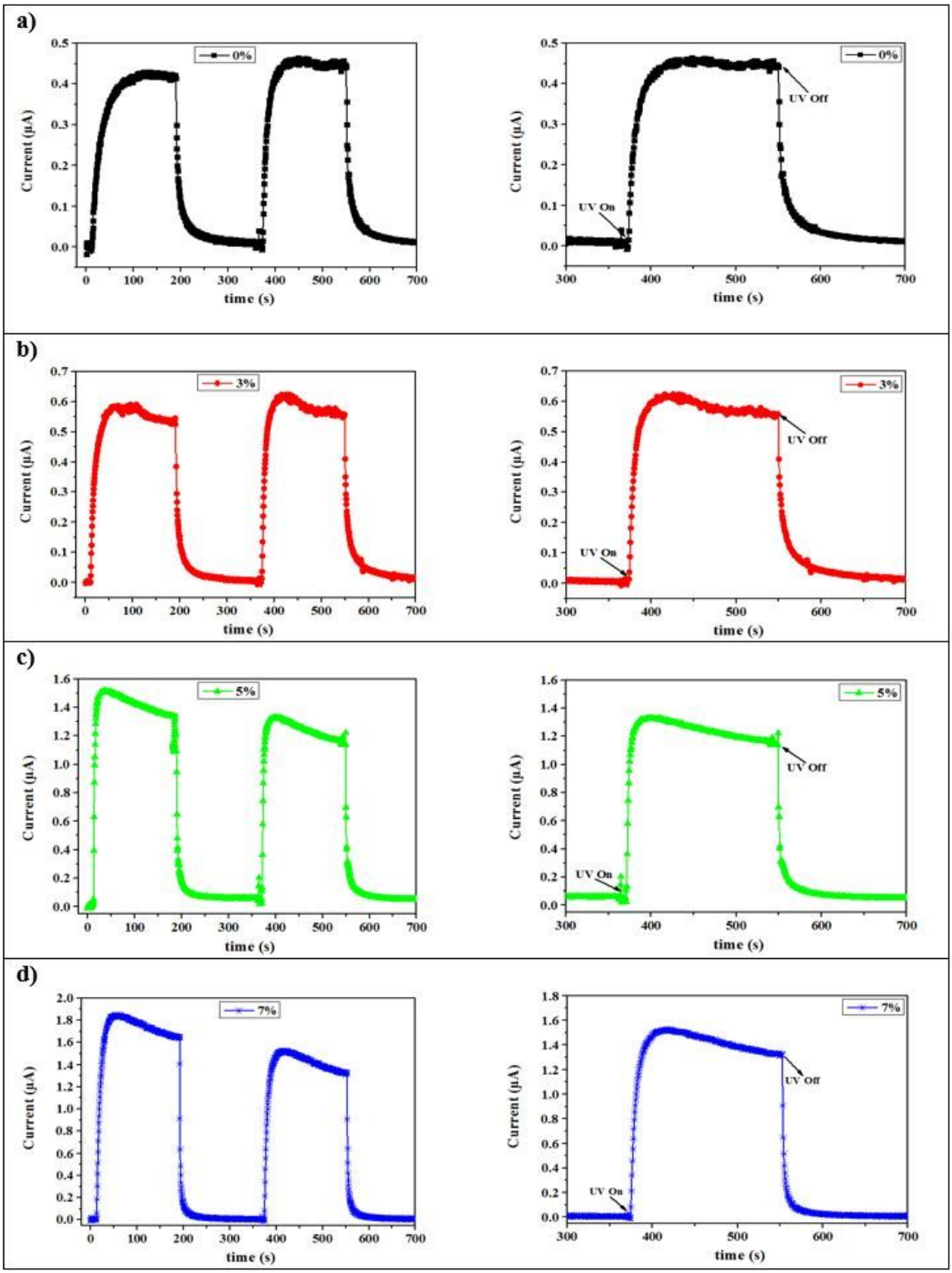

Figure 7

The I-t specification of the ZnO and ZnO:Cd nanostructures at different Cd concentrations (a) 0%, b) 3%, c) 5% and d) 7% measured with and without UV light illumination at 5 V.

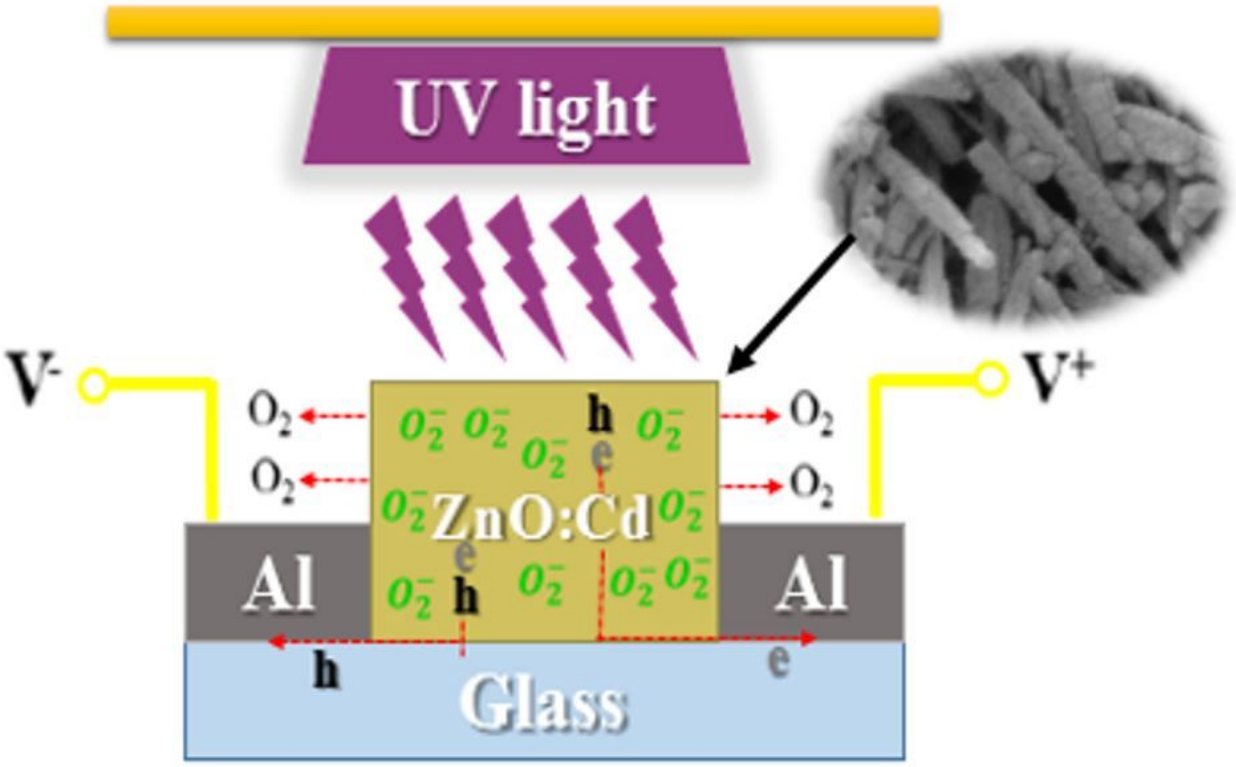

Figure 8

Schematic diagram of the ZnO:Cd nanorod photodetectors under UV radiation.